A CONSTITUTIVE MODEL FOR SHAPE MEMORY ALLOYS CONSIDERING TENSILE-COMPRESSIVE ASYMMETRY

Alberto Paiva
Arthur Martins Barbosa Braga
Pontifícia Universidade Católica do Rio de Janeiro
Departamento de Engenharia Mecânica
22.453.900 - Rio de Janeiro - RJ

Marcelo Amorim Savi
Universidade Federal do Rio de Janeiro
COPPE - Department of Mechanical Engineering
21.945.970 - Rio de Janeiro - RJ - Brazil, Caixa Postal 68.503
E-Mail: savi@ufrj.br

Abstract*. Shape Memory Alloys (SMAs) are materials that present, among other characteristics, the capacity to undergo large permanent deformations, and then, after a proper increase on the temperature, recover its original shape. Constitutive models consider phenomenological aspects of thermomechanical behavior of these alloys. The present contribution proposes a constitutive model to consider the tensile-compressive asymmetry that occurs in the mechanical behavior of SMAs. Numerical results show that the model is capable to capture the general behavior of SMAs, allowing the description of this important characteristic. A comparison between numerical and experimental results shows a good agreement.*

Keywords: *Shape memory alloys, Constitutive model, Tensile-compressive asymmetry.*

1. INTRODUCTION

Metallurgical studies have revealed the microstructural aspects of the behavior of SMAs (Otsuka & Ren, 1999; Shaw & Kyriakides, 1995). Basically, there are two possible phases on SMAs: austenite and martensite. In martensitic phase, there are plates that may be internally twin-related. Hence, different deformation orientations of crystallographic plates constitute what is known by martensitic variants. On SMAs there are 24 possible martensitic variants that are arranged in 6 plate groups with 4 plate variants per group (Zhang *et al*., 1991). Schroeder & Wayman (1977) have shown that when a specimen is deformed bellow a temperature where only martensitic phase is stable, with increasing stress, only one of the 4 variants in a given plate group will begin to grow. This variant is the one that has the largest partial shear stress. On the other hand, because the crystal structure of martensite is less symmetric than the austenite, only a single variant is created on the reverse transformation (Zhang *et al*., 1991). For the analysis of one-dimensional media, it is possible to consider only three variants of martensite together with austenite (A) on SMAs: the twinned martensite (M), which is stable in the absence of a stress field, and two other martensitic phases ($M+$, $M-$), which are induced by positive and negative stress fields, respectively.

Experimental results also show that SMAs present an asymmetric behavior when subjected to tensile or compressive loads. Polycrystalline NiTi, for example, deformed under compression presents smaller recoverable strain levels, higher critical transformation stress levels, and steeper transformation stress-strain slopes (Gall *et al.*, 1999). Gall & Sehitoglu (1999) argued that the tension-compression asymmetry in polycrystalline NiTi is caused by asymmetry at the single crystal level. Therefore, single crystal SMAs are expected to exhibit an extremely large tension-compression asymmetry since their martensite habit planes present a very low symmetry with respect to the parent phase.

Other important phenomenon related to SMAs thermomechanical behavior is the plasticity. Plastic strains are concerned in different articles in order to evaluate either effects of these strains in phase transformations or the description of the two-way shape memory effect (Miller & Lagoudas, 2000). The loss of actuation through repeated cycling due to plastic strain development is one of the important aspects related to the effect of plastic strains in SMAs.

The thermomechanical behavior of shape memory alloys may be modeled either by microscopic or macroscopic point of view. There are many different works dedicated to the constitutive description of the thermomechanical behavior of shape memory alloys, however, this is not a well established topic (James, 2000; Savi *et al.*, 2002).

This article presents a constitutive model for the description of the thermomechanical behavior of SMAs. The proposed model is based on the Fremond's theory (Fremond, 1987, 1996), later modified by Savi *et al.* (2002) and Baêta-Neves *et al.* (2003). Here, the tensile-compressive asymmetry is concerned allowing a correct description of the thermomechanical response of SMAs. The model here proposed includes four phases in the formulation: three variants of martensite and an austenitic phase. Plastic strain is included into the model and hardening effect is represented by a combination of kinematic and isotropic behaviors. An iterative numerical procedure based on the operator split technique (Ortiz *et al.*, 1983), the orthogonal projection algorithm and the return mapping algorithm (Simo & Hughes, 1998) is developed. Numerical results are carried out showing good agreements with experimental data.

2. CONSTITUTIVE MODEL

Fremond (1987, 1996) has proposed a three-dimensional model for the thermomechanical response of SMA where martensitic transformations are described with the aid of two internal variables. These variables represent volumetric fractions of two variants of martensite ($M+$ and $M-$), and must satisfy constraints regarding the coexistence of three distinct phases, the third being the parent austenitic phase (A). Savi *et al.* (2002) proposes a constitutive model built up on the original Fremond's model including a fourth phase related to twinned martensite (M). Moreover, the proposed model introduces the description of plastic strain, considering a thermo-plastic-phase transformation coupling. Recently, Baêta-Neves *et al.* (2003) proposes an enlargement of the stress-strain hysteresis loop in order to allow better adjustment to experimental data.

Modeling of SMA behavior can be done within the scope of the standard generalized material (Lemaitre & Chaboche, 1990). With this assumption, the thermomechanical behavior can be described by the Helmholtz free energy, ψ, and the pseudo-potential of dissipation, ϕ. The thermodynamic state is completely defined by a finite number of state variables: deformation, ε, temperature, T, the volumetric fractions of martensitic variants, β_1 and β_2, which are associated with detwinned martensites ($M+$ and $M-$, respectively) and austenite (A), β_3. The fourth phase is associated with twinned martensite (M) and its volumetric fraction is β_4. The plastic phenomenon is described with the aid of plastic strain, ε_p, and the hardening effect is represented by a combination of kinematic and isotropic behaviors, described by variables μ and γ, respectively. With these assumptions, each phase have a free energy function as follows,

$$M+: \quad \rho\psi_1(\varepsilon_e,T,\gamma,\mu)=\frac{1}{2}E_M\,\varepsilon_e^{\,2}-\alpha^T\varepsilon_e-\frac{L_M^{\,T}}{T_M}(T-T_M)-\Omega_M(T-T_0)\varepsilon_e+\frac{1}{2}K_M\,\gamma^2+\frac{1}{2H_M}\mu^2 \quad (1)$$

$$M-: \quad \rho\psi_2(\varepsilon_e,T,\gamma,\mu)=\frac{1}{2}E_M\,\varepsilon_e^{\,2}+\alpha^C\varepsilon_e-\frac{L_M^{\,C}}{T_M}(T-T_M)-\Omega_M(T-T_0)\varepsilon_e+\frac{1}{2}K_M\,\gamma^2+\frac{1}{2H_M}\mu^2 \quad (2)$$

$$A: \quad \rho\psi_3(\varepsilon_e,T,\gamma,\mu)=\frac{1}{2}E_A\,\varepsilon_e^{\,2}-\frac{L_A}{T_M}(T-T_M)-\Omega_A(T-T_0)\varepsilon_e+\frac{1}{2}K_A\,\gamma^2+\frac{1}{2H_A}\mu^2 \quad (3)$$

$$M: \quad \rho\psi_4(\varepsilon_e,T,\gamma,\mu)=\frac{1}{2}E_M\,\varepsilon_e^{\,2}+\frac{L_M}{T_M}(T-T_M)-\Omega_M(T-T_0)\varepsilon_e+\frac{1}{2}K_M\,\gamma^2+\frac{1}{2H_M}\mu^2 \quad (4)$$

where α, $L_M = L_M(T)$ and $L_A = L_A(T)$ are material parameters that describe martensitic transformation, E_M and E_A represent the elastic moduli for martesitic and austenitic phases, respectively; Ω_M and Ω_A represent the thermal expansion coefficient for martensitic and austenitic phases, respectively; K_M and K_A are the plastic moduli for martensitic and austenitic phases while H_M and H_A are the kinematic hardening moduli for martensitic and austenitic phases; T_M is a temperature below which the martensitic phase becomes stable in the absence of stress while T_0 is a reference temperature; ρ is the density. It should be pointed out that superscript T is related to tensile parameters while C is associated with compressive parameters. A free energy for the mixture can be written as follows,

$$\rho\,\hat{\psi}\left(\varepsilon_e, T, \gamma, \mu, \beta_1, \beta_2, \beta_3, \beta_4\right) = \rho \sum_{i=1}^{4} \beta_i\, \psi_i\left(\varepsilon_e, T, \gamma, \mu\right) + \hat{\mathbf{J}}\left(\beta_1, \beta_2, \beta_3, \beta_4\right) \tag{5}$$

where the volumetric fraction of the phases must satisfy constraints regarding the coexistence of four distinct phases:

$$0 \le \beta_i \le 1 \ (i=1,2,3,4)\ ; \quad \beta_1+\beta_2+\beta_3+\beta_4 = 1 \tag{6}$$

In the absence of stress, detwinned martensites, $M+$ and $M-$, do not exist. In order to include this physical aspect, an additional constraint must be written,

$$\beta_1 = \beta_2 = 0 \ \text{ if } \sigma = 0 \text{ and } \ \beta_1^S = \beta_2^S = 0 \tag{7}$$

where β_1^S and β_2^S are the values of β_1 and β_2, respectively, when the phase transformation begins to take place. With these considerations, $\hat{\mathbf{J}}$ is the indicator function of the convex τ (Rockafellar, 1970):

$$\tau = \left\{ \beta_i \in \Re \;\middle|\; \begin{array}{l} 0 \le \beta_i \le 1 \left(i = 1, 2, 3, 4\right); \beta_1 + \beta_2 + \beta_3 + \beta_4 = 1; \\ \beta_1 = \beta_2 = 0 \ \text{ if } \sigma = 0 \text{ and } \ \beta_1^S = \beta_2^S = 0 \end{array} \right\} \tag{8}$$

Using constraints (6), β_4 can be eliminated and the free energy can be rewritten as:

$$\rho\psi\left(\varepsilon, T, \beta_1, \beta_2, \beta_3, \varepsilon^p, \gamma, \mu\right) = \rho\tilde{\psi}\left(\varepsilon, T, \beta_1, \beta_2, \beta_3, \varepsilon^p, \gamma, \mu\right) + \mathbf{J}\left(\beta_1, \beta_2, \beta_3\right) \tag{9}$$

where,

$$\begin{aligned} \rho\tilde{\psi}\left(\varepsilon_e, T, \gamma, \mu, \beta_1, \beta_2, \beta_3\right) &= \beta_1\left[-\alpha^T\varepsilon_e - \frac{\left(L_M + L_M{}^T\right)}{T_M}\left(T - T_M\right)\right] + \beta_2\left[\alpha^C\varepsilon_e - \frac{\left(L_M + L_M{}^C\right)}{T_M}\left(T - T_M\right)\right] + \\ &+ \beta_3\ \left[\frac{1}{2}\left(E_A - E_M\right)\varepsilon_e{}^2 - \frac{\left(L_A + L_M\right)}{T_M}\left(T - T_M\right) - \left(\Omega_A - \Omega_M\right)\left(T - T_0\right)\varepsilon_e + \right. \\ &\left. + \frac{1}{2}\left(K_A - K_M\right)\gamma^2 + \left(\frac{1}{2H_A} - \frac{1}{2H_M}\right)\mu^2\right] + \\ &+ \frac{1}{2}E_M\,\varepsilon_e{}^2 + \frac{L_M}{T_M}\left(T - T_M\right) - \Omega_M\left(T - T_0\right)\varepsilon_e + \frac{1}{2}K_M\,\gamma^2 + \frac{1}{2H_M}\mu^2 + \mathbf{J}\left(\beta_1, \beta_2, \beta_3\right) \end{aligned} \tag{10}$$

Now, assuming additive decomposition, it is possible to write:

$$\varepsilon_e = \varepsilon - \varepsilon_p + \alpha_h^{\,C}\beta_2 - \alpha_h^{\,T}\beta_1 \tag{11}$$

Therefore, the free energy is rewritten as follows:

$$\begin{aligned}
&\rho\tilde{\psi}\left(\varepsilon,\varepsilon_p,T,\gamma,\mu,\beta_1,\beta_2,\beta_3\right) = \beta_1\left[-\alpha^T\left(\varepsilon-\varepsilon_p+\alpha_h^{\,C}\beta_2-\alpha_h^{\,T}\beta_1\right)-\frac{\left(L_M+L_M^{\,T}\right)}{T_M}\left(T-T_M\right)\right]+\\
&+\beta_2\left[\alpha^{c}\left(\varepsilon-\varepsilon_p+\alpha_h^{\,C}\beta_2-\alpha_h^{\,T}\beta_1\right)-\frac{\left(L_M+L_M^{\,C}\right)}{T_M}\left(T-T_M\right)\right]+\\
&+\beta_3\left[\frac{1}{2}\left(E_A-E_M\right)\left(\varepsilon-\varepsilon_p+\alpha_h^{\,C}\beta_2-\alpha_h^{\,T}\beta_1\right)^2-\frac{\left(L_A+L_M\right)}{T_M}\left(T-T_M\right)-\right.\\
&\left.-\left(\Omega_A-\Omega_M\right)\left(T-T_0\right)\left(\varepsilon-\varepsilon_p+\alpha_h^{\,C}\beta_2-\alpha_h^{\,T}\beta_1\right)+\frac{1}{2}\left(K_A-K_M\right)\gamma^2+\left(\frac{1}{2H_A}-\frac{1}{2H_M}\right)\mu^2\right]+\\
&+\frac{1}{2}E_M\left(\varepsilon-\varepsilon_p+\alpha_h^{\,C}\beta_2-\alpha_h^{\,T}\beta_1\right)^2+\frac{L_M}{T_M}\left(T-T_M\right)-\Omega_M\left(T-T_0\right)\left(\varepsilon-\varepsilon_p+\alpha_h^{\,C}\beta_2-\alpha_h^{\,T}\beta_1\right)+\\
&+\frac{1}{2}K_M\gamma^2+\frac{1}{2H_M}\mu^2+\mathbf{J}\left(\beta_1,\beta_2,\beta_3\right)
\end{aligned} \tag{12}$$

Now, **J** represents the indicator function of the tetrahedron π of the set (Figure 1),

$$\pi = \left\{\beta_i \in \Re \,\middle|\, \begin{array}{l} 0 \le \beta_i \le 1\,(i=1,2,3);\ \beta_1,\beta_2,\beta_3 \le 1 \\ \beta_1 = \beta_2 = 0 \text{ if } \sigma = 0 \text{ and } \beta_1^S = \beta_2^S = 0 \end{array}\right\} \tag{13}$$

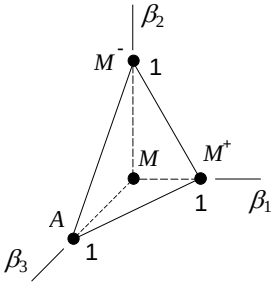

Figure 1 - Tetrahedron of the constraints π.

State equations can be obtained from the Helmholtz free energy as follows:

$$\sigma = \rho\frac{\partial\psi}{\partial\varepsilon} = E\left(\varepsilon-\varepsilon_p+\alpha_h^{\,C}\beta_2-\alpha_h^{\,T}\beta_1\right)+\alpha^{c}\beta_2-\alpha^{T}\beta_1-\Omega\left(T-T_0\right) \tag{14}$$

$$\begin{aligned}
B_1 \in -\rho\partial_1\psi = {} & \alpha^{T}\left(\varepsilon-\varepsilon_p\right)+\frac{\left(L_M+L_M^{\,T}\right)}{T_M}\left(T-T_M\right)+\beta_2\left(\alpha_h^{\,C}\alpha^{T}+\alpha_h^{\,T}\alpha^{c}+E\alpha_h^{\,T}\alpha_h^{\,C}\right)-\\
& -\beta_1\left(2\alpha_h^{\,T}\alpha^{T}+E\alpha_h^{\,T2}\right)+\alpha_h^{\,T}\left[E\left(\varepsilon-\varepsilon_p\right)-\Omega\left(T-T_0\right)\right]-\partial_1\mathbf{J}
\end{aligned} \tag{15}$$

$$\begin{aligned}
B_2 \in -\rho\partial_2\psi = {} & -\alpha^{c}\left(\varepsilon-\varepsilon_p\right)+\frac{\left(L_M+L_M^{\,C}\right)}{T_M}\left(T-T_M\right)+\beta_1\left(\alpha_h^{\,T}\alpha^{c}+\alpha_h^{\,C}\alpha^{T}+E\alpha_h^{\,C}\alpha_h^{\,T}\right)-\\
& -\beta_2\left(2\alpha_h^{\,C}\alpha^{c}+E\alpha_h^{\,C2}\right)-\alpha_h^{\,C}\left[E\left(\varepsilon-\varepsilon_p\right)-\Omega\left(T-T_0\right)\right]-\partial_2\mathbf{J}
\end{aligned} \tag{16}$$

$$B_3 \in -\rho\partial_3\psi = -\frac{1}{2}\left(E_A - E_M\right)\left(\varepsilon - \varepsilon_p + \alpha_h^C\beta_2 - \alpha_h^T\beta_1\right)^2 + \frac{\left(L_A + L_M\right)}{T_M}\left(T - T_M\right) + \\ + \left(\Omega_A - \Omega_M\right)\left(T - T_0\right)\left(\varepsilon - \varepsilon_p + \alpha_h^C\beta_2 - \alpha_h^T\beta_1\right) - \frac{1}{2}\left(K_A - K_M\right)\gamma^2 - \\ - \left(\frac{1}{2H_A} - \frac{1}{2H_M}\right)\mu^2 - \partial_3\mathbf{J} \tag{17}$$

$$X = -\frac{\partial\psi}{\partial\varepsilon_p} = E\left(\varepsilon - \varepsilon_p + \alpha_h^C\beta_2 - \alpha_h^T\beta_1\right) + \alpha^c\beta_2 - \alpha^r\beta_1 - \Omega\left(T - T_0\right) = \sigma \tag{18}$$

$$Y = -\rho\frac{\partial\psi}{\partial\gamma} = -K\gamma \tag{19}$$

$$Z = -\rho\frac{\partial\psi}{\partial\mu} = -\frac{1}{H}\mu \tag{20}$$

where B_i, X, Y and Z are the thermodynamic forces and σ represents the uniaxial stress; ∂_i is the *sub-differential* with respect to β_i (Rockafellar, 1970). Lagrange multipliers offer a good alternative to represent sub-differentials of the indicator function (Savi & Braga, 1993b). Furthermore, the parameters E, Ω, K and H are defined from their values in the austenitic and martensitic phase as follows:

$$(\bullet) = (\bullet)_M - \beta_3[(\bullet)_M - (\bullet)_A] \tag{21}$$

In order to describe the dissipation processes, it is necessary to introduce a pseudo-potential of dissipation. This pseudo-potential can be written through its dual ϕ^*. Considering the following type,

$$\phi^* = \frac{1}{2\eta_1}(B_1 + \eta_{ci}Y + \eta_{ck}Z)^2 + \frac{1}{2\eta_2}(B_2 + \eta_{ci}Y + \eta_{ck}Z)^2 + \frac{1}{2\eta_3}(B_3 - \eta_{ci}Y - \eta_{ck}Z)^2 + I_f \tag{22}$$

where I_f is the indicator function related to the yield surface defined as follows,

$$f = \left|X + HZ\right| - (\sigma_Y - Y) \quad \text{or} \quad f(\sigma,\mu,\gamma) = \left|\sigma - \mu\right| - (\sigma_Y + K\gamma) \tag{23}$$

The parameter η_i (i = 1,2,3) is associated with the internal dissipation of the material while η_{ci} and η_{ck} are related to plastic-phase transformation coupling. The parameter η_{ci} is associated with isotropic hardening coupling while η_{ck} is associated with kinematic hardening coupling. At this point, it is possible to write the following complementary equations:

$$\dot{\beta}_1 \in \partial_{B_1}\phi = \frac{B_1}{\eta_1} + \frac{\eta_{ci}}{\eta_1}Y + \frac{\eta_{ck}}{\eta_1}Z = \frac{B_1}{\eta_1} - \frac{\eta_{ci}}{\eta_1}K\gamma - \frac{\eta_{ck}}{\eta_1}\frac{\mu}{H} \tag{24}$$

$$\dot{\beta}_2 \in \partial_{B_2}\phi = \frac{B_2}{\eta_2} + \frac{\eta_{ci}}{\eta_2}Y + \frac{\eta_{ck}}{\eta_2}Z = \frac{B_2}{\eta_2} - \frac{\eta_{ci}}{\eta_2}K\gamma - \frac{\eta_{ck}}{\eta_2}\frac{\mu}{H} \tag{25}$$

$$\dot{\beta}_3 \in \partial_{B_3}\phi = \frac{B_3}{\eta_3} - \frac{\eta_{ci}}{\eta_3}Y - \frac{\eta_{ck}}{\eta_3}Z = \frac{B_3}{\eta_3} + \frac{\eta_{ci}}{\eta_3}K\gamma + \frac{\eta_{ck}}{\eta_3}\frac{\mu}{H} \tag{26}$$

$$\dot{\varepsilon}_p \in \partial_X\phi = \lambda\,\text{sign}\left(X + HZ\right) = \lambda\,\text{sign}\left(\sigma - \mu\right) \tag{27}$$

$$\dot{\gamma} \in \partial_Y\phi = \lambda + \eta_{ci}\left(\dot{\beta}_1 + \dot{\beta}_2 - \dot{\beta}_3\right) = \left|\dot{\varepsilon}_p\right| + \eta_{ci}\left(\dot{\beta}_1 + \dot{\beta}_2 - \dot{\beta}_3\right) \tag{28}$$

$$\dot{\mu} \in \partial_Z \phi = \lambda H \text{ sign}\left(X + HZ\right) + \eta_{ck}\left(\dot{\beta}_1 + \dot{\beta}_2 - \dot{\beta}_3\right) = H\,\dot{\varepsilon}_p + \eta_{ck}\left(\dot{\beta}_1 + \dot{\beta}_2 - \dot{\beta}_3\right) \tag{29}$$

where λ is the plastic multiplier. The irreversible nature of plastic flow is represented by means of the *Kuhn-Tucker conditions*. Another constraint must be satisfied when $f(\sigma,\gamma,\mu)=0$. It is referred to as the *consistency condition* and corresponds to the physical requirement that a stress point on the yield surface must persist on it. These conditions are presented as follows (Simo & Hughes, 1998):

$$\lambda \geq 0\,;\;\; f(\sigma,\gamma,\mu) \leq 0\,;\;\; \lambda\, f(\sigma,\gamma,\mu) = 0\;\;;\;\; \lambda\, \dot{f}(\sigma,\gamma,\mu) = 0 \text{ if } f(\sigma,\gamma,\mu) = 0 \tag{30}$$

These equations form a complete set of constitutive equations. Since the pseudo-potential of dissipation is convex, positive and vanishes at the origin, the Clausius-Duhen inequality is automatically satisfied if the entropy is defined as $s = -\partial\psi / \partial T$.

Furthermore, it is important to consider the definition of the parameters $L_M = L_M(T)$ and $L_A = L_A(T)$, which are obtained assuming $\dot{\beta}_1 = 0$ and $\varepsilon = \varepsilon_R$ in a critical temperature, T_C, below which there is no change in stress-strain hysteresis loop position. With this aim, it is necessary to define the following parameters for tensile behavior,

$$\alpha_h^{\,T} = \varepsilon_R^{\,T} - \frac{\alpha_{\tau}}{E_M} - \frac{\Omega_M}{E_M}\left(T_C^{\,T} - T_0\right) \qquad T_C^T = T_M\left[\frac{\left(L + L_M^T\right)E_M - \alpha_{\tau}^{\,2} + \alpha_{\tau}\,\Omega_M\,T_0}{\left(L + L_M^T\right)E_M + \alpha_{\tau}\,\Omega_M\,T_M}\right] \tag{31}$$

Analogous, it is necessary to define similar parameters for compressive behavior:

$$\alpha_h^{\,C} = -\varepsilon_R^{\,C} - \frac{\alpha_{c}}{E_M} + \frac{\Omega_M}{E_M}\left(T_C^{\,C} - T_0\right) \qquad T_C^C = T_M\left[\frac{\left(L + L_M^C\right)E_M - \alpha_{c}^{\,2} - \alpha_{c}\,\Omega_M\,T_0}{\left(L + L_M^C\right)E_M - \alpha_{c}\,\Omega_M\,T_M}\right] \tag{32}$$

Hence, using these conditions in Equations (24) e (25), the following expressions are obtained,

$$L_M(T) = \begin{cases} L_M = L\,, & \text{if} \quad T \geq T_C \\ L_M = L\,\dfrac{\left(T_C - T_M\right)}{\left(T - T_M\right)}, & \text{if} \quad T < T_C \end{cases} \qquad L_A(T) = \begin{cases} L_A = L\,, & \text{if} \quad T \geq T_C \\ L_A = 2L - \left[L\,\dfrac{\left(T_C - T_M\right)}{\left(T - T_M\right)}\right], & \text{if} \quad T < T_C \end{cases} \tag{33}$$

Moreover, in order to contemplate different characteristics to the kinetics of phase transformation for loading and unloading processes, it is possible to consider different values to the parameter η_i, which is related to internal dissipation: η_i^L and η_i^U, being the internal dissipation parameters related to variable β_i during loading or unloading process, respectively.

The operator split technique (Ortiz *et al.*, 1983) associated with an iterative numerical procedure is developed in order to deal with the nonlinearities in the formulation. The procedure isolates the sub-differentials and uses the implicit Euler method combined with an orthogonal projection algorithm (Savi *et al.*, 2002) to evaluate evolution equations. Orthogonal projections assure that volumetric fractions of the phases will obey the imposed constraints. In order to satisfy constraints expressed in (13), values of volumetric fractions must stay inside or on the boundary of π, the tetrahedron shown in Figure 1. The elasto-plastic behavior is simulated with the aid of the return mapping algorithm proposed by Simo & Hughes (1998).

3. NUMERICAL SIMULATIONS

In order to evaluate the response predicted by the proposed model, a SMA specimen is subjected to different thermomechanical loadings. Basically, stress-driving simulations are carried out considering tensile and compressive behaviors at a constant temperature. Moreover, it is assumed that all simulations are performed without reaching the yield surface.

Experimental results presented by Gall *et al.* (1999) are used as reference to validate the numerical results obtained from the proposed model. In the experimental tests developed in the cited reference, single and polycrystal specimens with different orientation and subjected to different aging treatments are analyzed. The aging treatment causes Ti_3Ni_4 precipitation, being related to the tension-compression asymmetry. Basically, these precipitates act as nucleation sites for martensite and obstacles for dislocation motion. This mechanism effectively increases the critical stress for dislocation motions and decreases the critical stress for phase transformation.

Table 1. Thermomechanical properties: Peak-aged single crystal [111] orientation, aged 1.5h at 673K.

E_A (GPa)	E_M (GPa)	α^T (MPa)	α^C (MPa)	ε_R^T	ε_R^C
36.5	107	4044	1520	0.0646	–0.0227

L (MPa)	L_M^T (MPa)	L_M^C (MPa)
152	–120	87.5

Ω_A (MPa/K)	Ω_M (MPa/K)	T_M (K)	T_A (K)	T_0 (K)
0.74	0.17	273.5	317.5	295

η_1^L (MPa.s)	η_1^U (MPa.s)	η_2^L (MPa.s)	η_2^U (MPa.s)	η_3^L (MPa.s)	η_3^U (MPa.s)
6.02	6.02	4.09	4.09	3.8	3.8

Table 2. Thermomechanical properties: Over-aged single crystal. [111] orientation, aged 15h at 773K.

E_A (GPa)	E_M (GPa)	α^T (MPa)	α^C (MPa)	ε_R^T	ε_R^C
94	161	2250	1670	0.0723	–0.0311

L (MPa)	L_M^T (MPa)	L_M^C (MPa)
152	–85	40

Ω_A (MPa/K)	Ω_M (MPa/K)	T_M (K)	T_A (K)	T_0 (K)
0.74	0.17	271.2	301.7	295

η_1^L (MPa.s)	η_1^U (MPa.s)	η_2^L (MPa.s)	η_2^U (MPa.s)	η_3^L (MPa.s)	η_3^U (MPa.s)
1.91	1.91	2.063	2.063	2	2

Here, numerical simulations related to some of these tests are carried out, showing the potentiality of the proposed model. At first, a single crystal aged 1.5h at 673K (peak aged) is considered. The parameters presented in Table 1 are used for numerical simulations. Under this condition, compressive behavior presents small values of critical stress, where phase transformation begins to take place, and also smaller residual strains. The model response captures this behavior as shown in Figure 2a. On the other hand, tensile behavior is quite different. Numerical and experimental results are in agreement except for the response during unloading in tensile behavior. Gall *et al.* (1999) say that this indicates that transformation product is unstable under tensile unloading.

Figure 2b shows the same test related to a different aging treatment, namely aged 15h at 773K (over-aged), which the specimen is subjected before the test. Table 2 presents the employed parameters. Again, experimental and numerical results are in agreements. Notice that aging treatment alters the response of the specimen changing the slope of the phase transformation region. Gall *et al.* (1999) say that either tension-compression asymmetry or orientation dependence of the stress-strain response are strongly related to heat treatments (precipitate sizes).

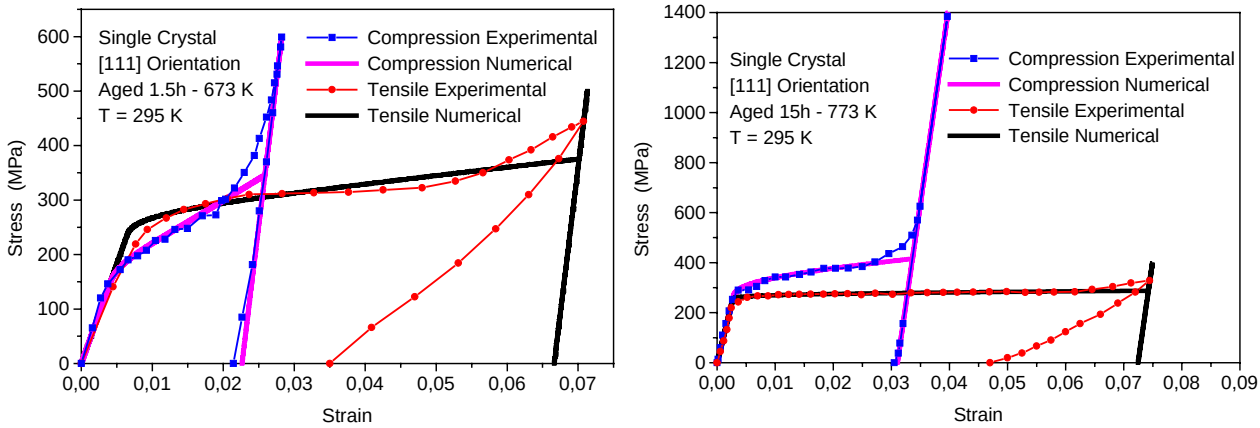

Figure 2 – Stress-strain curves for a single crystal with [111] orientation:
(a) aged 1.5h at 673K. (b) aged 15h at 773K.

Table 3. Thermomechanical properties: Peak-aged polycrystal
<111> {110} texture, aged 1.5h at 673K.

E_A (GPa)	E_M (GPa)	α^T (MPa)	α^C (MPa)	ε_R^T	ε_R^C
58	96.5	1817	910	0.0525	–0.0268

L (MPa)	L_M^T (MPa)	L_M^C (MPa)
120	–69	76

Ω_A (MPa/K)	Ω_M (MPa/K)	T_M (K)	T_A (K)	T_0 (K)
0.74	0.17	262.2	314	295

η_1^L (MPa.s)	η_1^U (MPa.s)	η_2^L (MPa.s)	η_2^U (MPa.s)	η_3^L (MPa.s)	η_3^U (MPa.s)
5.7	5.7	6.75	6.75	7	7

Table 4. Thermomechanical properties: Over-aged polycrystal <111> {110} texture, aged 15h at 773K.

E_A (GPa)	E_M (GPa)	α^T (MPa)	α^C (MPa)	ε_R^T	ε_R^C
78	148	1880	1443	0.0536	–0.0262

L (MPa)	L_M^T (MPa)	L_M^C (MPa)
100	–60	27

Ω_A (MPa/K)	Ω_M (MPa/K)	T_M (K)	T_A (K)	T_0 (K)
0.74	0.17	273.8	305.8	295

η_1^L (MPa.s)	η_1^U (MPa.s)	η_2^L (MPa.s)	η_2^U (MPa.s)	η_3^L (MPa.s)	η_3^U (MPa.s)
3.24	3.24	3.58	3.58	3.3	3.3

The forthcoming analysis considers a polycrystal SMA with <111> {110} texture (Figure 3). Results are qualitatively similar to the previous one related to single crystals. Since the proposed model is related to phenomenological features, the results demonstrate the model ability in describing both single and polycrystals behavior. Table 3 presents parameters used for the peak-aged polycrystal specimen. Figure 3a shows the numerical simulation together with experimental data. Notice that the numerical and experimental results are in good agreement as well as in the single crystals simulations.

Finally, Figure 3b shows results related to an over-aged polycrystal. Parameters are presented in Table 4. Again, results present qualitatively the same behavior compared to the related single crystal response, showing quantitative agreements between numerical and experimental data. Both results associated with polycrystal simulations are analogous showing a smaller influence of the aging process in the thermomechanical behavior.

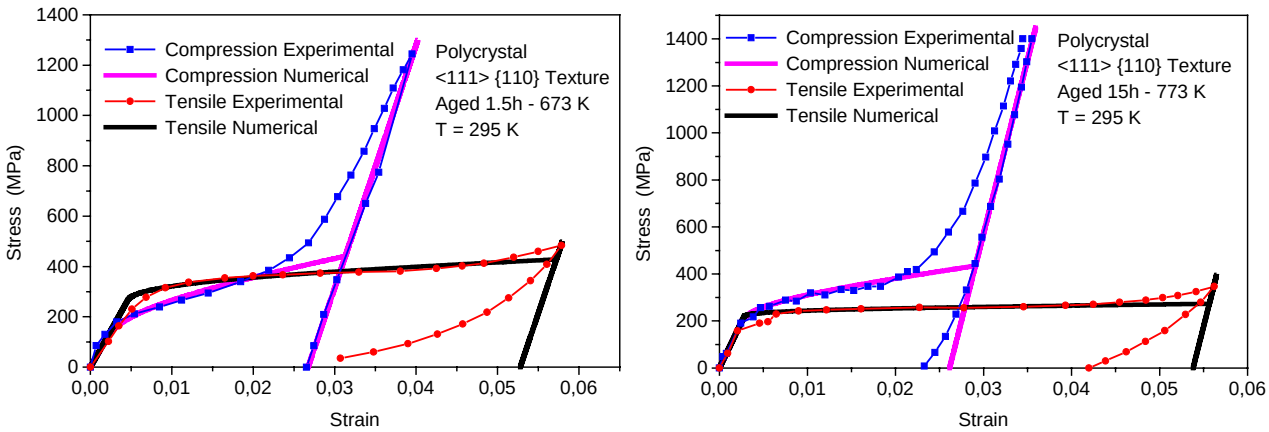

Figure 3 – Stress-strain curves for a polycrystal with <111> {110} texture. (a) aged 1.5h at 673K. (b) aged 15h at 773K.

4. CONCLUSIONS

The description of the thermomechanical behavior of SMAs involves different and complex phenomena. Among others, plastic strain and thermo-plastic-phase transformation coupling are some of these behaviors. This article proposes a constitutive model that is capable to describe the tensile-compressive asymmetry. Numerical and experimental results are in agreement showing the potentiality of the proposed model.

5. REFERENCES

Baêta-Neves, A.P., Savi, M.A. & Pacheco, P.M.C.L., 2003, "Horizontal Enlargement of the Stress-Strain Loop on a Thermo-Plastic-Phase Transformation Coupled Model for Shape Memory Alloys", Proceedings of *COBEM 2003 - 17th International Congress of Mechanical Engineering*, São Paulo, Brazil.

Fremond, M., 1987, "Matériaux à Mémoire de Forme", *C.R. Acad. Sc. Paris*, Tome 34, s.II, n.7, pp. 239-244.

Fremond, M., 1996, "*Shape Memory Alloy: A Thermomechanical Macroscopic Theory*", CISM courses and lectures, Springer Verlag.

Gall, K., Sehitoglu, H, Chumlyakov, Y.I. & Kireeva, I.V., 1999, "Tension-Compression Asymmetry of the Stress-Strain Response in Aged Single Crystal and Polycrystalline NiTi", *Acta Mater.*, v.47, n.4, pp.1203-1217.

Gall, K. & Sehitoglu, H., 1999, "The Role of Texture in Tension-Compression Asymmetry in Polycrystalline NiTi", *International Journal of Plasticity*, v.15, pp.69-92.

James, R.D., 2000, "New Materials from Theory: Trends in the Development of Active Materials", *International Journal of Solids and Structures*, v.37, pp.239-250.

Lemaitre, J. & Chaboche, J.-L., 1990, "*Mechanics of Solid Materials*", Cambridge University Press.

Miller, D.A. & Lagoudas, D.C., 2000, "Thermo-mechanical Characterization of NiTiCu and NiTi SMA Actuators: Influence of Plastic Strains", *Smart Materials & Structures*, v.5, pp.640-652.

Ortiz, M., Pinsky, P.M. & Taylor, R.L., 1983, "Operator Split Methods for the Numerical Solution of the Elastoplastic Dynamic Problem", *Computer Methods of Applied Mechanics and Engineering*, v.39, pp.137-157.

Otsuka, K. & Ren, X., 1999, "Recent developments in the research of Shape Memory Alloys", *Intermetallics*, v.7, pp.511-528.

Rockafellar, R. T., 1970, "*Convex Analysis*", Princeton Press.

Savi, M.A. & Braga, A.M.B., 1993, "Chaotic Vibrations of an Oscillator with Shape Memory", *Journal of the Brazilian Society for Mechanical Sciences*, v.XV, n.1, pp.1-20, 1993.

Savi, M. A., Paiva, A., Baêta-Neves, A. P. & Pacheco, P. M. C. L., 2002, "Phenomenological Modeling and Numerical Simulation of Shape Memory Alloys: A Thermo-Plastic-Phase Transformation Coupled Model", *Journal of Intelligent Material Systems and Structures*, v.3, n.5, pp.261-273.

Schroeder, T.A. & Wayman, C.M., 1977, "The Formation of Martensite and the Mechanism of the Shape Memory Effect in Single Crystals of Cu-Zn Alloys", *ACTA Metallurgica*, v.25, pp.1375.

Shaw, J. A. & Kyriakides, S., 1995, "Thermomechanical Aspects of NiTi", *Journal of Mechanics Physics Solids*, v.43, pp.1243-1281.

Simo, J.C. & Hughes, T.J.R., 1998, "*Computational Inelasticity*", Springer.

Zhang, X.D., Rogers, C.A. & Liang, C., 1991, "Modeling of Two-Way Shape Memory Effect", *ASME - Smart Structures and Materials*, v.24, pp.79-90.